Biointerface Research in Applied Chemistry
Open-Access Journal (ISSN: 2069-5837)

Article
Volume 13, Issue 2, 2023, 139
https://doi.org/10.33263/BRIAC132.139

Mathematical Transformation of Multidimensional Correlated Data into Uncorrelated Raman Spectra to Increase the Sensitivity of Identification with Silver Nanoparticles

Viktor M. Emelyanov [1,*], Tatiana A. Dobrovolskaya [1], Viktor V. Yemelyanov [1]

[1] The Southwest State University; Faculty of Mechanics and Technology, Kursk, Russia vmemelianov@yandex.ru (V.M.E.); dobtatiana74@mail.ru(T.A.D.); wemelyanov@yandex.ru (V.V.Y.);
* Correspondence: vmemelianov@yandex.ru (V.M.E);

Scopus Author ID 56344103500

Received: 29.12.2021; Accepted: 24.01.2022; Published: 25.03.2022

Abstract: The article discusses approaches to translating correlated statistical data into uncorrelated form. The results of the transformation of mathematical models with silver nanoparticles and without nanoparticles into uncorrelated form with simultaneous solution of a system of equations with uncorrelated matrices are presented. Solutions of a system of multi-dimensional equations for determining the probability densities p0 and p1 are obtained. These mathematical models are based on the Raman polarization spectra of polyester fibers in recognizing silver nanoparticles, taking into account the polarization of laser radiation in two directions: X-across and Y-along the fibers. A method for increasing the resolution of the identification of silver nanoparticles on polyester fibers is proposed. When solving the system using nonlinear quadratic and XY differential equations of probability densities of distribution ellipses, the resolution of identification of silver nanoparticles p0 and p1 in the range 10^{-2}- 10^{-547} was obtained.

Keywords: colloidal silver nanoparticles; Raman spectra; multi-dimensional correlation equations; the intersection of distribution ellipses; transformation of correlation data; recognition reliability; normal two-dimensional distributions; resolution of nanoparticle identification.

1. Introduction

To ensure nano, pico - and molecular biotechnology requires accuracy and resolution in the range of 10^{-9} - 10^{-16} mathematical models of data processing and technical devices.

Research data [1-5] have shown the possibility of signal amplification using Raman spectroscopy up to 10^{6} - 10^{7} using graphene [6-20] and silicon nanofibers. To increase the resolution, especially when detecting cancer cells [21-24], bilirubin [9, 15], combinations of various metal nanoparticles Ag, Au, Cu [11] are used to obtain plasmon effects on silicon wafers with surface modification by inhomogeneities in the form of vertical and horizontal nanofibers [12].

The prospect of increasing the resolution is estimated - identifying interdependencies between multi-dimensional parameters when processing a large number of statistical data [25,26].

The paper [14] revealed the possibility of constructing mathematical models and solving the problem of obtaining accuracy up to 10^{-16} - 10^{-18} using the construction of systems and solving systems with multi-dimensional correlation mathematical equations and taking into account the interdependence of parameters.

According to [27-30], the accuracy of solving multi-dimensional correlation mathematical equations in 10^{-14} - 10^{-16} in automatic mode has been consistently obtained for a long time. However, the resolution is not sufficient since data is obtained only in the range 10^{-1} - 10^{-7}. This is not acceptable since a resolution of 10^{-14} - 10^{-16} with the currently obtained accuracy is required when solving multi-dimensional correlation mathematical equations.

Many problems, in this case, are that the compilation and solution of systems of correlation equations requires a large number of such equations in the system, for example, up to 81 equations. Many equations are necessary to account for all significant 9 peaks of the Raman spectrum in two directions across X and along Y of the object of study. The compilation and solution of such several correlation equations in the system are impossible at this technical level. Therefore, a simplified compilation and solution of a system of such equations do not provide the required reliability.

In these studies, the Bayes hypothesis is used to multiply the obtained interdependent (correlation) probabilities:

$$P_0 = P_1/P_{1c} \cdot P_2/P_{2c} \cdot \ldots \cdot P_n/P_{nc}, \quad (1)$$

where P_0 is the total probability of occurrence of events; P_1/P_{1c}, P_2/P_{2c},, ..., P_n/P_{nc} are the probabilities of dependent (correlation) events [25,26].

However, it is almost impossible to obtain interdependent probabilities for a large number of parameters and compose and solve a multi-dimensional system of up to 81 equations. In [14, 27, 28, 30], solutions were obtained only for two-dimensional correlation mathematical models and [29] for three-dimensional ones.

Therefore, in order to apply the Bayes hypothesis for a large number of parameters, it is necessary to mathematically transform all interdependent (correlation) parameters into an independent (uncorrelated) form. Then you can use the Bayes hypothesis for independent probabilities:

$$P_0 = P_1 \cdot P_2 \cdot P_3 \cdot \ldots \cdot P_n, \quad (2)$$

where P_0 is the total probability of occurrence of events; P_1, P_2, P_3, ..., P_n are the probabilities of independent events.

Research in [31] aims to solve the problem of converting dependent (correlation) data into an independent form and vice versa from independent data into a dependent form. In these studies, the mathematical transformation into an independent form is performed simultaneously with the solution of a system of correlation multi-dimensional equations.

2. Materials and Methods

For clarity, the preliminary transformation of correlation data into an independent firm with the solution of the problem of detecting the intersection of ellipses of correlation and non-correlation data is shown in Figure 1 when generating correlation and non-correlation data according to the normal law of distribution ellipses using experimental data [31].

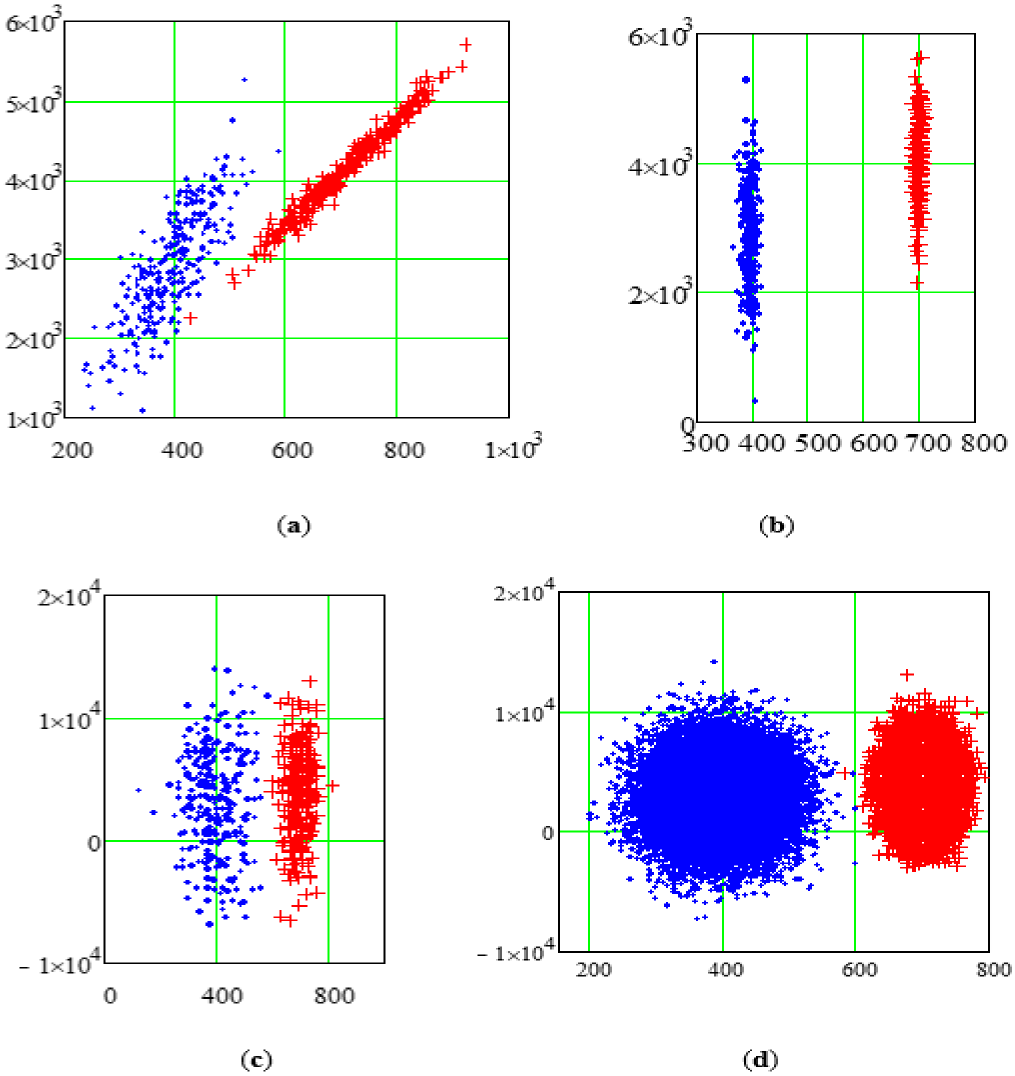

Figure 1. Mathematical transformation of the two-dimensional dependence (correlation) of the data in the independent (no correlation) when generated according to the normal law with the conservation and real parameters of the ellipses values of the peaks of the Raman spectrum of polyester fibers with silver nanoparticles (+ +) and without nanoparticles (· ·):(**a**) – 288 generate correlation data ellipses values of the peaks of the Raman spectrum;(**b**) – data conversion ellipses, Fig.1a in a non-correlative form with the preservation of mathematical expectations and mean square deviations;(**c**) - the change in Fig. 1b during the generation of mean square deviations up to the intersection with one point of the ellipses of the Raman spectrum with silver nanoparticles and without nanoparticles;(**d**) - generation of 28800 independent data of Raman spectrum ellipses with silver nanoparticles and without nanoparticles with an 8-fold increase in the values of mean square deviations to the intersection with one point of the Raman spectrum ellipses with silver nanoparticles and without nanoparticles.

The transformation is based on obtaining a diagonal matrix of eigenvalues λ0=eigenvals(rXY) from the correlation matrix rXY [31].

Finding the diagonal matrix of the eigenvalues of the correlation matrix is mathematically worked out in [31]. For example, for two-dimensional data for the correlation dependence on X and Y, when solving a specific problem of converting Raman spectra, we obtain:

$$\Sigma := \begin{pmatrix} 1 & rXY1_{i,j} \\ rXY1_{i,j} & 1 \end{pmatrix} \quad \mathrm{eigenvals}\begin{pmatrix} 1 & rXY1_{i,j} \\ rXY1_{i,j} & 1 \end{pmatrix} \rightarrow \begin{pmatrix} 1 - rXY1_{i,j} \\ rXY1_{i,j} + 1 \end{pmatrix} \quad \Sigma 1 := \begin{pmatrix} 1 - rXY1_{i,j} & 0 \\ 0 & 1 + rXY1_{i,j} \end{pmatrix}$$

Then the transformation of mathematical models with silver nanoparticles and without nanoparticles into an uncorrelated form with simultaneous solution of a system of equations with uncorrelated matrices will have the following form for Ag9-12 (i=0; j=4):

$$\sum 0 := \begin{pmatrix} 1 - rXY0_{i,j} & 0 \\ 0 & 1 + rXY0_{i,j} \end{pmatrix} \quad \sum 1 := \begin{pmatrix} 1 - rXY1_{i,j} & 0 \\ 0 & 1 + rXY1_{i,j} \end{pmatrix}$$

$$f(x,y) := \left[\begin{matrix} \left[\ln\left[\frac{1}{(2\cdot\pi)\cdot\left[\left(\left|\sum 1\right|\right)^{0.5}\right]}\right] + \frac{-1}{2}\cdot\left[\frac{x - MENX1_i}{\sigma\Delta X1_i} \quad \frac{y-0}{\sigma\Delta Y1_j}\right]\cdot\sum 1^{-1}\cdot\begin{pmatrix}\frac{x - MENX1_i}{\sigma\Delta X1_i} \\ \frac{y-0}{\sigma\Delta Y1_j}\end{pmatrix}\right] & 1 \\ \left[\ln\left[\frac{1}{(2\cdot\pi)\cdot\left[\left(\left|\sum 0\right|\right)^{0.5}\right]}\right] + \frac{-1}{2}\cdot\left[\frac{x - MENX0_i}{\sigma\Delta X0_i} \quad \frac{y-0}{\sigma\Delta Y0_j}\right]\cdot\sum 0^{-1}\cdot\begin{pmatrix}\frac{x - MENX0_i}{\sigma\Delta X0_i} \\ \frac{y-0}{\sigma\Delta Y0_j}\end{pmatrix}\right] & 1 \end{matrix}\right] \tag{3}$$

$$g(x,y) := \left[\begin{matrix} \frac{d}{dx}\left[\left(\frac{x - MENX1_1}{\sigma\Delta X1_i} \quad \frac{y-0}{\sigma\Delta Y1_j}\right)\cdot\sum 1^{-1}\cdot\begin{pmatrix}\frac{x - MENX1_1}{\sigma\Delta X1_i} \\ \frac{y-0}{\sigma\Delta Y1_j}\end{pmatrix}\right] & \frac{d}{dy}\left[\left(\frac{x - MENX1_1}{\sigma\Delta X1_i} \quad \frac{y-0}{\sigma\Delta Y1_j}\right)\cdot\sum 1^{-1}\cdot\begin{pmatrix}\frac{x - MENX1_1}{\sigma\Delta X1_i} \\ \frac{y-0}{\sigma\Delta Y1_j}\end{pmatrix}\right] \\ \frac{d}{dx}\left[\left(\frac{x - MENX0_1}{\sigma\Delta X0_i} \quad \frac{y-0}{\sigma\Delta Y0_j}\right)\cdot\sum 0^{-1}\cdot\begin{pmatrix}\frac{x - MENX0_1}{\sigma\Delta X0_i} \\ \frac{y-0}{\sigma\Delta Y0_j}\end{pmatrix}\right] & \frac{d}{dy}\left[\left(\frac{x - MENX0_1}{\sigma\Delta X0_i} \quad \frac{y-0}{\sigma\Delta Y0_j}\right)\cdot\sum 0^{-1}\cdot\begin{pmatrix}\frac{x - MENX0_1}{\sigma\Delta X0_i} \\ \frac{y-0}{\sigma\Delta Y0_j}\end{pmatrix}\right] \end{matrix}\right]$$

x:=610.0 y:=0

Given

f(x,y) = 0 g(x,y) = 0

v2:= Find(x,y) $v2 = \begin{pmatrix} 615.635489 \\ 0 \end{pmatrix}$

$f(v2_0, v2_1) = 5.664475168578822\times10^{-14}$ $g(v2_0, v2_1) = 0$

$$R0 := \left(\frac{v2_0 - MENX0_i}{\sigma\Delta X0_i} \quad \frac{v2_1 - 0}{\sigma\Delta Y0_j}\right)\cdot\sum 0^{-1}\cdot\begin{pmatrix}\frac{v2_0 - MENX0_i}{\sigma\Delta X0_i} \\ \frac{v2_1 - 0}{\sigma\Delta Y0_j}\end{pmatrix}$$

$$R1 := \left(\frac{v2_0 - MENX1_i}{\sigma\Delta X1_i} \quad \frac{v2_1 - 0}{\sigma\Delta Y1_j}\right)\cdot\sum 1^{-1}\cdot\begin{pmatrix}\frac{v2_0 - MENX1_i}{\sigma\Delta X1_i} \\ \frac{v2_1 - 0}{\sigma\Delta Y1_j}\end{pmatrix}$$

$$pQ0 := \frac{1}{(2\cdot\pi)\left[\left(\left|\sum 0\right|\right)^{0.5}\right]}\cdot e^{\frac{-1}{2}\cdot R0} \quad pQ1 := \frac{1}{(2\cdot\pi)\left[\left(\left|\sum 1\right|\right)^{0.5}\right]}\cdot e^{\frac{-1}{2}\cdot R1}$$

$pQ0 = 1.4884714041498341\times10^{-16}$

$pQ1 = 1.4884714041499187\times10^{-16}$

$QAg := \frac{1}{pQ0}$ $QAg = 6718301723580423$ $QAg = 6.718\times10^{15}$

The solution of the system of equations (3) gives the result:

$pQ0=1.4884714041498341\times10^{-16}$ and $pQ1=1.4884714041499187\times10^{-16}$, which is acceptable both in accuracy and resolution.

To verify the reliability, it is also necessary to evaluate the graphical representation of the intersection of the distribution ellipses of the Raman spectra of polyester fibers with silver nanoparticles and without nanoparticles.

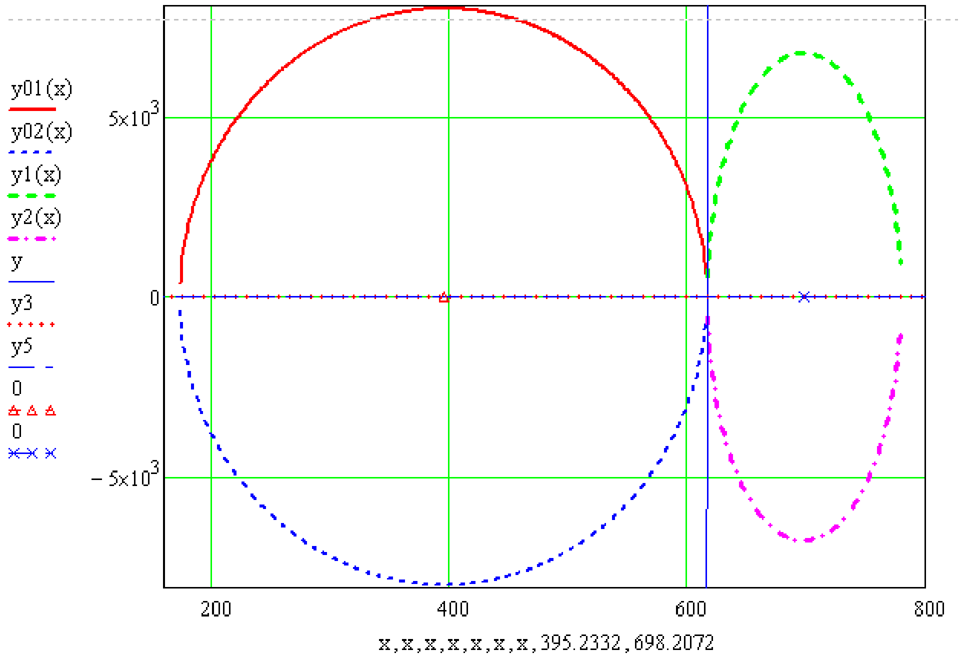

Figure 2. Validation by graphical representation of the intersection of ellipses of the distribution of Raman spectra of polyester fibers with silver nanoparticles and without nanoparticles

It is also necessary to check the likelihood of the intersection of the distribution ellipses with correlated and uncorrelated peak values in experiments on Raman spectra. Instead of binding to the axis $MENY0_j=0$ and $MENU1_j=0$ according to (3) Figure 2, we use the solution (4) Figure 3 with binding to the axis $MENY0_j$ and $MENY1_j$:

$$f(x,y) := \begin{bmatrix} \left[\ln\left[\frac{1}{(2\cdot\pi)\cdot\left[\left(\left|\sum 1\right|\right)^{0.5}\right]}\right] + \frac{-1}{2}\cdot\left[\frac{x-MENX1_i}{\sigma\Delta X1_i} \quad \frac{y-MENY1_j}{\sigma\Delta Y1_j}\right]\cdot{\sum 1}^{-1}\cdot\begin{pmatrix}\frac{x-MENX1_i}{\sigma\Delta X1_i}\\ \frac{y-MENY1_j}{\sigma\Delta Y1_j}\end{pmatrix}\right] & 1 \\ \left[\ln\left[\frac{1}{(2\cdot\pi)\cdot\left[\left(\left|\sum 0\right|\right)^{0.5}\right]}\right] + \frac{-1}{2}\cdot\left[\frac{x-MENX0_i}{\sigma\Delta X0_i} \quad \frac{y-MENY0_j}{\sigma\Delta Y0_j}\right]\cdot{\sum 0}^{-1}\cdot\begin{pmatrix}\frac{x-MENX0_i}{\sigma\Delta X0_i}\\ \frac{y-MENY0_j}{\sigma\Delta Y0_j}\end{pmatrix}\right] & 1 \end{bmatrix} \quad (4)$$

$$g(x,y) := \begin{bmatrix} \frac{d}{dx}\left[\left(\frac{x-MENX1_1}{\sigma\Delta X1_i} \quad \frac{y-MENY1_j}{\sigma\Delta Y1_j}\right)\cdot{\sum 1}^{-1}\cdot\begin{pmatrix}\frac{x-MENX1_1}{\sigma\Delta X1_i}\\ \frac{y-MENY1_j}{\sigma\Delta Y1_j}\end{pmatrix}\right] & \frac{d}{dy}\left[\left(\frac{x-MENX1_1}{\sigma\Delta X1_i} \quad \frac{y-MENY1_j}{\sigma\Delta Y1_j}\right)\cdot{\sum 1}^{-1}\cdot\begin{pmatrix}\frac{x-MENX1_1}{\sigma\Delta X1_i}\\ \frac{y-MENY1_j}{\sigma\Delta Y1_j}\end{pmatrix}\right] \\ \frac{d}{dx}\left[\left(\frac{x-MENX0_1}{\sigma\Delta X0_i} \quad \frac{y-MENY0_j}{\sigma\Delta Y0_j}\right)\cdot{\sum 0}^{-1}\cdot\begin{pmatrix}\frac{x-MENX0_1}{\sigma\Delta X0_i}\\ \frac{y-MENY0_j}{\sigma\Delta Y0_j}\end{pmatrix}\right] & \frac{d}{dy}\left[\left(\frac{x-MENX0_1}{\sigma\Delta X0_i} \quad \frac{y-MENY0_j}{\sigma\Delta Y0_j}\right)\cdot{\sum 0}^{-1}\cdot\begin{pmatrix}\frac{x-MENX0_1}{\sigma\Delta X0_i}\\ \frac{y-MENY0_j}{\sigma\Delta Y0_j}\end{pmatrix}\right] \end{bmatrix}$$

x:=610.0 y:=3000

Given

f(x,y) = 0 g(x,y) = 0

v2:= Find(x,y) $v2 = \begin{pmatrix} 615.936996 \\ 03314.635572 \end{pmatrix}$

$f(v2_0, v2_1) = 5.692137786687368 \times 10^{-14}$ $\quad$ $g(v2_0, v2_1) = 3.58395868724902 \times 10^{-17}$

$$R0 := \begin{pmatrix} \dfrac{v2_0 - MENX0_i}{\sigma\Delta X0_i} & \dfrac{v2_1 - MENY0_j}{\sigma\Delta Y0_j} \end{pmatrix} \cdot \Sigma 0^{-1} \cdot \begin{pmatrix} \dfrac{v2_0 - MENX0_i}{\sigma\Delta X0_i} \\ \dfrac{v2_1 - MENY0_j}{\sigma\Delta Y0_j} \end{pmatrix}$$

$$R1 := \begin{pmatrix} \dfrac{v2_0 - MENX1_i}{\sigma\Delta X1_i} & \dfrac{v2_1 - MENY1_j}{\sigma\Delta Y1_j} \end{pmatrix} \cdot \Sigma 1^{-1} \cdot \begin{pmatrix} \dfrac{v2_0 - MENX1_i}{\sigma\Delta X1_i} \\ \dfrac{v2_1 - MENY1_j}{\sigma\Delta Y1_j} \end{pmatrix}$$

$$pQ0 := \frac{1}{(2 \cdot \pi)\left[(|\Sigma 0|)^{0.5}\right]} \cdot e^{\frac{-1}{2} \cdot R0} \quad pQ1 := \frac{1}{(2 \cdot \pi)\left[(|\Sigma 1|)^{0.5}\right]} \cdot e^{\frac{-1}{2} \cdot R1}$$

$pQ0 = 1.245798943704045 \times 10^{-16}$

$pQ1 = 1.2457980437041158 \times 10^{-16}$

$$QAg := \frac{1}{pQ0} \quad QAg = 8026983226163763 \quad QAg = 8.027 \times 10^{15}$$

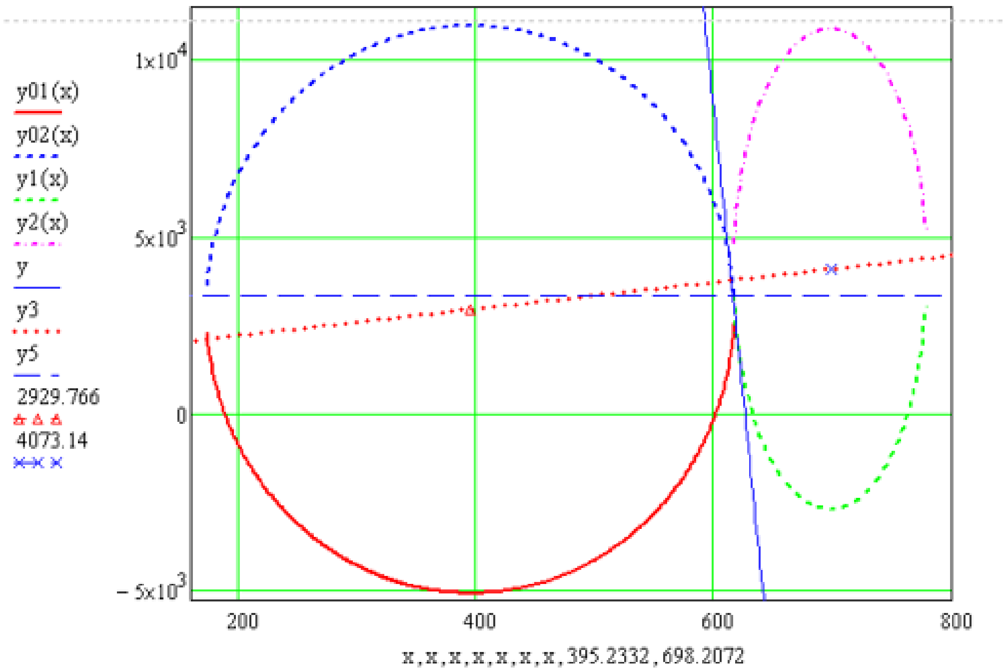

Figure 3. Graphical validation based on the image of the intersection of ellipses of the distribution of Raman spectra of polyester fibers with silver nanoparticles and without nanoparticles with reference to the $MENY0_j$ - $MENY1_j$ axis.

The solution of the system of equations (4) gives the result:

$pQ0=1.245798043704045 \times 10^{-16}$ and

$pQ1=1.2457980437041158 \times 10^{-16}$, which is acceptable both in accuracy and resolution.

To confirm, it is also necessary to evaluate the intersections of the distribution ellipses of the Raman spectra of polyester fibers with silver nanoparticles and without nanoparticles with the initial experimental correlated data with the results already obtained for (3) –(4):

$$\Sigma 0 := \begin{pmatrix} 1 & rXY0_{i,j} \\ rXY0_{i,j} & 1 \end{pmatrix} \quad \Sigma 1 := \begin{pmatrix} 1 & rXY1_{i,j} \\ rXY1_{i,j} & 1 \end{pmatrix}$$

$$f(x,y) := \left[\begin{matrix} \left[\ln\left[\frac{1}{(2\cdot\pi)\cdot\left[\left(\left|\sum 1\right|\right)^{0.5}\right]}\right] + \frac{-1}{2}\cdot\left[\frac{x-MENX1_i}{\sigma\Delta X1_i} \quad \frac{y-MENY1_j}{\sigma\Delta Y1_j}\right]\cdot\sum 1^{-1}\cdot\left(\begin{matrix}\frac{x-MENX1_i}{\sigma\Delta X1_i}\\ \frac{y-MENY1_j}{\sigma\Delta Y1_j}\end{matrix}\right)\right] & 1 \\ \left[\ln\left[\frac{1}{(2\cdot\pi)\cdot\left[\left(\left|\sum 0\right|\right)^{0.5}\right]}\right] + \frac{-1}{2}\cdot\left[\frac{x-MENX0_i}{\sigma\Delta X0_i} \quad \frac{y-MENY0_j}{\sigma\Delta Y0_j}\right]\cdot\sum 0^{-1}\cdot\left(\begin{matrix}\frac{x-MENX0_i}{\sigma\Delta X0_i}\\ \frac{y-MENY0_j}{\sigma\Delta Y0_j}\end{matrix}\right)\right] & 1 \end{matrix}\right] \tag{5}$$

$$g(x,y) := \left[\begin{matrix} \frac{d}{dx}\left[\left(\frac{x-MENX1_1}{\sigma\Delta X1_i} \quad \frac{y-MENY1_j}{\sigma\Delta Y1_j}\right)\cdot\sum 1^{-1}\cdot\left(\begin{matrix}\frac{x-MENX1_1}{\sigma\Delta X1_i}\\ \frac{y-MENY1_j}{\sigma\Delta Y1_j}\end{matrix}\right)\right] & \frac{d}{dy}\left[\left(\frac{x-MENX1_1}{\sigma\Delta X1_i} \quad \frac{y-MENY1_j}{\sigma\Delta Y1_j}\right)\cdot\sum 1^{-1}\cdot\left(\begin{matrix}\frac{x-MENX1_1}{\sigma\Delta X1_i}\\ \frac{y-MENY1_j}{\sigma\Delta Y1_j}\end{matrix}\right)\right] \\ \frac{d}{dx}\left[\left(\frac{x-MENX0_1}{\sigma\Delta X0_i} \quad \frac{y-MENY0_j}{\sigma\Delta Y0_j}\right)\cdot\sum 0^{-1}\cdot\left(\begin{matrix}\frac{x-MENX0_1}{\sigma\Delta X0_i}\\ \frac{y-MENY0_j}{\sigma\Delta Y0_j}\end{matrix}\right)\right] & \frac{d}{dy}\left[\left(\frac{x-MENX0_1}{\sigma\Delta X0_i} \quad \frac{y-MENY0_j}{\sigma\Delta Y0_j}\right)\cdot\sum 0^{-1}\cdot\left(\begin{matrix}\frac{x-MENX0_1}{\sigma\Delta X0_i}\\ \frac{y-MENY0_j}{\sigma\Delta Y0_j}\end{matrix}\right)\right] \end{matrix}\right]$$

$x:=400.0$ $\qquad$ $y:=2000$

Given

$f(x,y) = 0 \quad g(x,y) = 0$

$v2 := \mathrm{Find}(x,y) \qquad v2 = \begin{pmatrix} 449.955654 \\ 2471.429168 \end{pmatrix}$

$f(v2_0,v2_1) = -3.504467994814062\times10^{-15} \qquad g(v2_0,v2_1) = -5.142505384808134\times10^{-18}$

$$R0 := \left(\frac{v2_0-MENX0_i}{\sigma\Delta X0_i} \quad \frac{v2_1-MENY0_j}{\sigma\Delta Y0_j}\right)\cdot\sum 0^{-1}\cdot\left(\begin{matrix}\frac{v2_0-MENX0_i}{\sigma\Delta X0_i}\\ \frac{v2_1-MENY0_j}{\sigma\Delta Y0_j}\end{matrix}\right)$$

$$R1 := \left(\frac{v2_0-MENX1_i}{\sigma\Delta X1_i} \quad \frac{v2_1-MENY1_j}{\sigma\Delta Y1_j}\right)\cdot\sum 1^{-1}\cdot\left(\begin{matrix}\frac{v2_0-MENX1_i}{\sigma\Delta X1_i}\\ \frac{v2_1-MENY1_j}{\sigma\Delta Y1_j}\end{matrix}\right)$$

$$pQ0 := \frac{1}{(2\cdot\pi)\left[\left(\left|\sum 0\right|\right)^{0.5}\right]}\cdot e^{\frac{-1}{2}\cdot R0} \qquad pQ1 := \frac{1}{(2\cdot\pi)\left[\left(\left|\sum 1\right|\right)^{0.5}\right]}\cdot e^{\frac{-1}{2}\cdot R1}$$

$pQ0 = 0.01100562484527942$

$pQ1 = 0.01100562484527937$

$QAg := \frac{1}{pQ0} \qquad QAg = 90.863$

To verify the reliability, it is also necessary to evaluate the graphical representation of the intersection of the ellipses of the distribution of Raman spectra of polyester fibers with silver nanoparticles and without nanoparticles with the initial experimental correlated data:

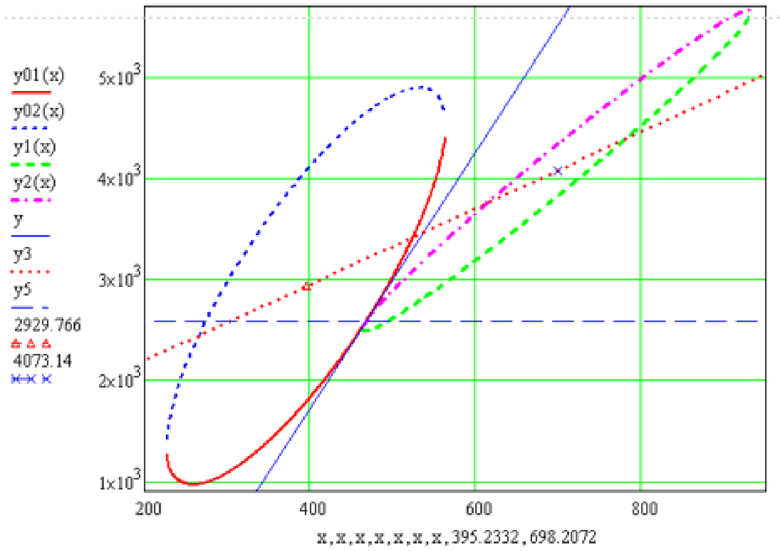

Figure 4. Graphical representation of the intersection of ellipses of the distribution of Raman spectra of polyester fibers with silver nanoparticles and without nanoparticles according to the initial experimental correlation data

3. Results and Discussion

The general results of solving the problem for all peaks from i=0...8 to j=0...8 in total 81 equations with mathematically transformed uncorrelated statistical data of the Raman spectrum of polyester fiber with silver nanoparticles are shown in the following figures.

$$Q := \begin{pmatrix} 4.174\times10^{7} & 60.33 & 3.285\times10^{6} & 2.821\times10^{13} & 4.719\times10^{4} & 2.383\times10^{10} & 2.178\times10^{4} & 1.518\times10^{4} & 2.661\times10^{4} \\ 7.401\times10^{6} & 51.585 & 9.875\times10^{5} & 5.493\times10^{12} & 1.038\times10^{5} & 1.89\times10^{9} & 1.956\times10^{4} & 1.467\times10^{4} & 2.969\times10^{4} \\ 2.313\times10^{8} & 73.165 & 1.668\times10^{6} & 5.088\times10^{12} & 4.971\times10^{4} & 1.432\times10^{10} & 1.765\times10^{4} & 1.178\times10^{4} & 2.53\times10^{4} \\ 1.148\times10^{8} & 62.512 & 6.549\times10^{6} & 2.681\times10^{14} & 7.068\times10^{4} & 9.32\times10^{10} & 3.417\times10^{4} & 1.57\times10^{4} & 3.626\times10^{4} \\ 6.718\times10^{15} & 134.957 & 8.431\times10^{10} & 7.756\times10^{26} & 1.913\times10^{6} & 2.527\times10^{17} & 1.661\times10^{6} & 1.084\times10^{5} & 1.3\times10^{6} \\ 6.458\times10^{7} & 62.176 & 4.171\times10^{6} & 5.373\times10^{13} & 6.134\times10^{4} & 3.453\times10^{10} & 2.525\times10^{4} & 1.824\times10^{4} & 3.345\times10^{4} \\ 1.164\times10^{16} & 162.902 & 7.979\times10^{9} & 7.305\times10^{21} & 5.062\times10^{5} & 3.874\times10^{16} & 3.062\times10^{5} & 7.743\times10^{4} & 5.986\times10^{5} \\ 2.309\times10^{3} & 26.681 & 2.645\times10^{3} & 5.147\times10^{5} & 1.151\times10^{3} & 3.87\times10^{4} & 372.607 & 8.025\times10^{4} & 1.124\times10^{4} \\ 2.335\times10^{4} & 32.165 & 3.159\times10^{4} & 2.824\times10^{8} & 1.151\times10^{3} & 2.154\times10^{6} & 1.393\times10^{3} & 1.99\times10^{5} & 5.461\times10^{4} \end{pmatrix}$$

Figure 5. Matrix of the results of assessing the reliability of the intersection of the ellipses of the distribution of Raman spectra of polyester fibers with silver nanoparticles and without nanoparticles according to statistical data converted to uncorrelated form.

$$QL_{i,j} := \log(Q_{i,j})$$

$$QL = \begin{pmatrix} 7.621 & 1.781 & 6.517 & 13.45 & 4.674 & 10.377 & 4.338 & 4.181 & 4.425 \\ 6.869 & 1.713 & 5.995 & 12.74 & 5.016 & 9.276 & 4.291 & 4.166 & 4.473 \\ 8.364 & 1.864 & 6.222 & 12.707 & 4.696 & 10.156 & 4.247 & 4.071 & 4.403 \\ 8.06 & 1.796 & 6.816 & 14.428 & 4.849 & 10.969 & 4.534 & 4.196 & 4.559 \\ 15.827 & 2.13 & 10.926 & 26.89 & 6.282 & 17.403 & 6.22 & 5.035 & 6.114 \\ 7.81 & 1.794 & 6.62 & 13.73 & 4.788 & 10.538 & 4.402 & 4.261 & 4.524 \\ 16.066 & 2.212 & 9.902 & 21.864 & 5.704 & 16.588 & 5.486 & 4.889 & 5.777 \\ 3.363 & 1.426 & 3.422 & 5.712 & 3.061 & 4.588 & 2.571 & 4.904 & 4.051 \\ 4.368 & 1.507 & 4.5 & 8.451 & 3.061 & 6.333 & 3.144 & 5.299 & 4.737 \end{pmatrix}$$

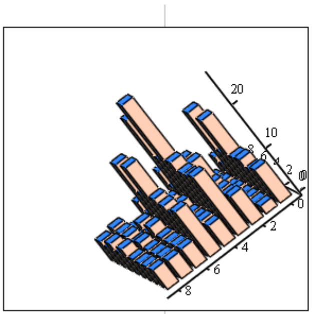

QL

Figure 6. Data of logarithmic values of the reliability of the intersection of ellipses of the distribution of Raman spectra of polyester fibers with silver nanoparticles and without nanoparticles according to the results of conversion to uncorrelated form.

The total value of the sum of logarithms of confidence with silver nanoparticles and without nanoparticles according to the results of conversion to uncorrelated form:

$$SQL := \sum_{j=0}^{8}\sum_{i=0}^{8} QL_{i,j} \quad SQL = 547.123 \quad SQL1 := \frac{SQL}{81} \quad SQL1 = 6.755$$

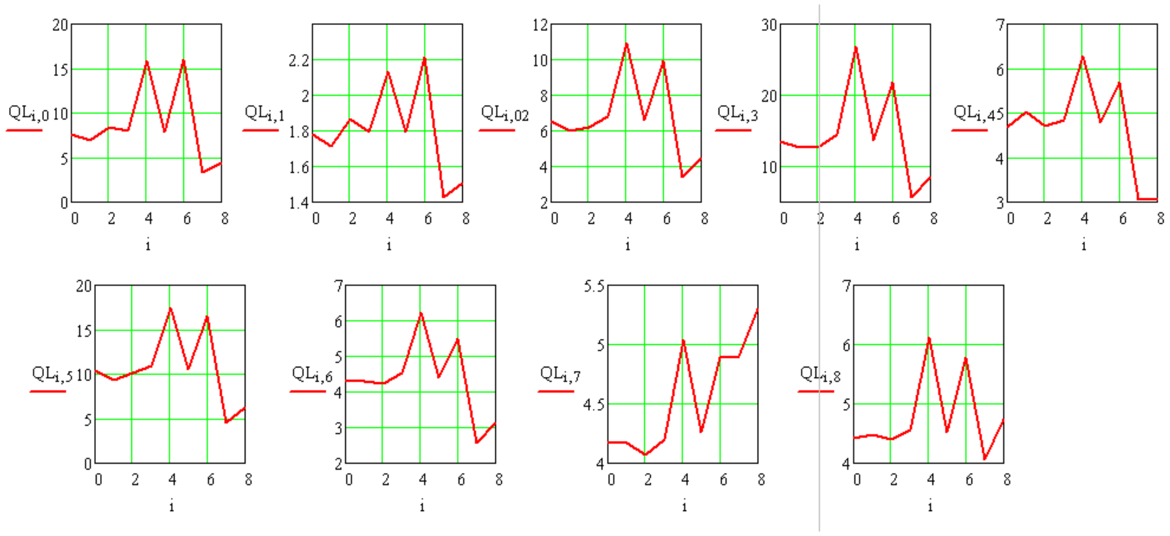

Figure 7. The logarithm of the confidence of the intersection of the ellipses of the distribution of Raman spectra of polyester fibers with silver nanoparticles and without nanoparticles in columns j=0 - 8 of the matrix of logarithmic confidence values Figure 6.

4. Conclusions

The use of a mathematical method for converting statistical correlation data into an uncorrelated form while simultaneously solving a system of equations for multi-dimensional Raman spectra of polyester fibers without nanoparticles and with silver nanoparticles makes it possible to increase the sensitivity of nanosilver identification up to 10^{547} times and, consequently, increase the resolution of the method.

The method uses the possibilities of applying the Bayes hypothesis when multiplying the probability densities in the intersection of the ellipses of the distribution of the values of the peaks of the Raman spectra of polyester with silver nanoparticles without nanoparticles with transformed correlated statistical data in an uncorrelated form.

The transformation of correlated statistical data into an uncorrelated form is carried out on the basis of finding diagonal matrices from eigenvalues (numbers) correlation matrices used to compile systems of equations.

This study selected correlation matrices of two-dimensional parameters: X - across the fibers and Y -along the fibers. The transformation and solution equations system is designed to replace the traditional ellipse equation with a vector-matrix form using a diagonal matrix of eigenvalues, which allows uncorrelated transformations and simultaneous rotations and displacement of the coordinate axes of the ellipses to the origin of the coordinates MENY0 and MENY1. As a result, the values of probability densities for the transformed uncorrelated transformed data for the peak with i=0 and j=4 were obtained: $pQ1=1.4884714041498341\cdot10^{-16}$ or the inverse value (confidence) $QAg=6.718\cdot10^{15}$ compared to the original correlated data: pQ1= 0. 01100562484527942 with the inverse value (Q-factor) QAg=90.863. These results for comparison are also obtained in this article.

A system of equations has also been compiled and solved for conversion to an uncorrelated form with the ellipses of distributions bound to the axes: MENY0, MENX0 –

MENY1, MENX1. The values obtained are:pQ1=1.2457980437041158 $\cdot 10^{-16}$ or the inverse value (confidence) QAg=8.027$\cdot 10^{15}$.

A matrix of all 81 values of Q and log Q is also obtained. Since when multiplying all the independent terms of the matrix Q, we get 10^{547}, i.e., more than 10^{307} than the computing capabilities of a conventional computer, we have to use logarithmic values of the terms of the matrix log Q. In this case, all the values of the terms are added for the log Q matrix, and the sum value 547 is obtained. For one member of this matrix, we get an average value of 6.755 or $10^{6.755}$ =5.683$\cdot 10^{6}$.

Further research aims to compile and solve a system of equations for converting correlated data into uncorrelated data for different concentrations of deposited colloidal silver: 5% and 11%, to compare with 17% of the already proven research method in this work.

Funding

This research received no external funding.

Acknowledgments

This research has no acknowledgment.

Conflicts of Interest

The authors declare no conflict of interest.

References

1. Schedin, F.; Lidorikis, E.; Lombardo, A.; Kravets, V. G.; Geim, A.K.; Grigorenko, A.N.; Novoselov, K.S.; Ferrari, A.C. Surface enhanced raman spectroscopy of graphene.*ACS Nano* **2010,** *4*, 5617-5626,https://doi.org/10.1021/nn1010842.
2. Andryukov, B.G.; Karpenko, A.A.; Matosova, E.V.; Lyapun, I.N. *CTM* **2019**, *11*, 161-174,http://doi.org/10.17691/stm2019.11.4.19.
3. Yaminskiy, I.V.; Sinitsyna, O.V.; Akhmetova, A.I.; Senotrusova, S.A.; Piryazev, A.A.; Kozhina,E.P.; Bedin S.A. Use of microlenses to improve the optical microscopy resolution and enhance Raman scattering. *Nanoindustry* **2021**, *6*, http://doi.org/10.22184/1993-8578.2021.14.6.382.388.
4. Daoudi, K.; Gaidi, M.; Columbus, S. Silver nanoprisms/graphene oxide/silicon nanowires composites for R6G surface-enhanced Raman spectroscopy sensor. *Biointerface Research in Applied Chemistry* **2020**, *10*, 5670-5674, https://doi.org/10.33263/briac103.670674.
5. Yujia, L.; Hanzheng, X.; Jingyi Xu. Synthesis and Applications of Functional Nanomaterials. *Journal of Physics: Conference Series* **2021**, *2133*, https://doi.org/10.1088/1742-6596/2133/1/012006.
6. Kukushkin, V.I.; Grishina, Ya.V.; Solov'ev, V.V.; Kukushkin, I.V. Size plasmon–polariton resonance and its contribution to the giant enhancement of the Raman scattering. *JETP Letters* **2017**, *105*, 677-681, https://doi.org/10.1134%2FS0021364017100071.
7. Langer, J.; et al. Present and future of surface-enhanced Raman scattering. *ACS Nano* **2020**, *14*, 28−117, https://doi.org/10-1021/acsnano.9b04224.
8. Turkoglu, E.A.; Bakhshpour, M.; Denizli, A. Molecularly imprinted biomimetic surface plasmon resonance sensor for hormone detection. *Biointerface Research in Applied Chemistry* **2019**, *9*, 4090-4095, https://doi.org/10.33263/briac94.090095.
9. Xu, D.; Duan, L.; Jia, W.; Yang, G.; Gu, Y. Fabrication of Ag@Fe2O3 hybrid materials as ultrasensitive SERS substrates for the detection of organic dyes and bilirubin in human blood. *Microchemical Journal* **2021**, *161*,https://doi.org/10.1016/j.microc.2020.105799.
10. Saviñon-Flores, F.; Méndez, E.; López-Castaños, M.; Carabarin-Lima, A.; López-Castaños, K.A.; González-Fuentes, M.A.; Méndez-Albores, A. A. Review on SERS-Based Detection of Human Virus Infections: Influenza and Coronavirus. *Biosensors* **2021**, *11*, https://doi.org/10.3390/bios11030066.

11. Rouhbakhsh, H;Farkhari, N.;Ahmadi-kandjani, S.;Karima, S.;Tajalli, H.;Rashidi, M.A. Low-Cost Stable SERS Substrate Based on Modified Silicon Nanowires. *Plasmonics* **2019**, *14*, 869–874,https://doi.org/10.1007/s11468-018-0868-2.
12. Alhmoud, H.; Brodoceanu, D.; Elnathan, R.; Kraus, T.; Voelcker, N. H. A MACEing silicon: Towards single-step etching of defined porous nanostructures for biomedicine. *Prog. Mater. Sci*. **2021**, *116*, 100636, https://doi.org/10.1016/j.pmatsci.2019.100636.
13. Ningbo, Yi; Chen, Z.; Qinghai, S.; Shumin, X. A hybrid system with highly enhanced graphene SERS for rapid and tag-free tumor cells detection. *Scientific Reports***2016**,*6*, https://doi.org/10.1038/srep25134.
14. Emelyanov, V. M.; Dobrovolskaya, T. A.; Emelyanov, V. V.Multidimensional system of equations with XY-Y differentiation of probability densities p0-p1 for identification of gold nanoparticles. *Biointerface Research in Applied Chemistry* **2018**, *8*, 3652-3656, http://dx.doi.org/10.1088/1757-899X/905/1/012014.
15. Kartashova, A.D.; Gonchar, K.A.; Chermoshentsev, D.A.; Alekseeva, E.A.; Gongalsky, M.B.; Bozhev, I.I.; Eliseev, A.A.; Dyakov, S.A.; Samsonova, J.V.; Osminkina, L.A. Surface-Enhanced Raman Scattering-Active Gold-Decorated SiliconNanowire Substrates for Label-Free Detection of Bilirubin. *ACS Biomaterials Science & Engineering***2021**,https://doi.org/10.1021/acsbiomaterials.1c00728.
16. Shvaly, V.; Filipič, G.; Zavašnik, J.; Abdulhalim, I.; Cvelbar, U. Surface-enhanced Raman spectroscopy for chemical and biological sensing using nanoplasmonics: The relevance of interparticle spacing and surface morphology. *Applied Physics Reviews***2020**,*7*,https://doi.org/10.1063/5.0015246.
17. Sealy, C. Rotated graphene stacks up for better membranes. *Nano Today* **2021**, *37*, https://doi.org/10.1016/j.nantod.2021.101116.
18. Afanas'ev, V.P.; Lobanova, L.G.; Selyakov, D.N.; Semenov-Shefov, M.A. Effect of nanocoating morphology on the signal of X-ray Photoelectron Spectroscopy. *Journal of Physics: Conference Series* **2021**, *2144*, https://doi.org/10.1088/1742-6596/2144/1/012007.
19. Wang, W.; Zhou, L.; Li, Ya.; Li, P.; Chen, G.; Yang, Sh. Study on the Ablation Properties of Nano-graphite Modified EPDM Insulators. *Journal of Physics: Conference Series* **2021**, *2133*, https://doi.org/10.1088/1742-6596/2133/1/012019.
20. Tu Phan, Le M.; Thu Vo, T. A.; Hoang, Thi X.; Cho, S. Graphene Integrated Hydrogels Based Biomaterials in Photothermal Biomedicine. *Nanomaterials* **2021**, *11*, 906, https://doi.org/10.3390/nano11040906.
21. Gomes, H. I. O.; Martins, C. S. M.; Prior, João A. V. Silver Nanoparticles as Carriers of Anticancer Drugs for Efficient Target Treatment of Cancer Cells. *Nanomaterials* **2021**, *11*, 964, https://doi.org/10.3390/nano11040964.
22. Zhang, M.; Dai, Z.; Theivendran, Sh.; Gu, Zh.; Zhao, L.; Song, H.; Yang, Y. Nanotechnology enabled reactive species regulation in biosystems for boosting cancer immunotherapy. *Nano Today* **2021**, *36*, 101035, https://doi.org/10.1016/j.nantod.2020.101035.
23. Levit, Sh. L.; Tang, Ch. Polymeric Nanoparticle Delivery of Combination Therapy with Synergistic Effects in Ovarian Cancer. *Nanomaterials* **2021**, *11*, 1048, https://doi.org/10.3390/nano11041048.
24. Wu, Ch.; Wu, Yi.; Zhu, X.; Zhang, J.; Liu, J.; Zhang, Y. Near-infrared-responsive functional nanomaterials: the first domino of combined tumor therapy. *Nano Today* **2021**, *36*,https://doi.org/10.1016/j.nantod.2020.100963.
25. Han, N.; Ram, R.J. Bayesian modeling and computation for analyte quantification in complex mixtures using Raman spectroscopy. *Computational Statistics & Data Analysis* **2020**, *143*, 106846, https://doi.org/10.1016/j.csda.2019.106846.
26. Härkönen, T.; Roininen, L.; Moores, M.T.; Vartiainen, E.M.Bayesian Quantification for Coherent Anti-Stokes Raman Scattering Spectroscopy. *J. Phys. Chem. B* **2020**, *124*, 7005–7012, https://doi.org/10.1021/ACS.JPCB.0C04378.
27. Emelyanov, V.M.; Dobrovolskaya, T.A.; Emelyanov, V.V. Automatic Solution of the System of Equations of the Equivalent Radius of the Distribution Ellipses of Dielectric Materials for the Recognition of Gold Nanoparticles, 2021 International Seminar on Electron Devices Design and Production (SED), Prague, Czech Republic, 27-28 April 2021; Publisher: IEEE *Xplore*, **2021**, 20800604, https://doi.org/10.1109/SED51197.2021.9444524.
28. Dobrovolskaya, T.A.; Emelyanov, V.M.; Emelyanov, V.V. Improving the Accuracy of the Solution of a Multi-dimensional System by Differentiating the XY Probability Density Equations for the Identification of Gold Nanoparticles on Fibers, 2020 Moscow Workshop on Electronic and Networking Technologies (MWENT), Moscow, Russia, 1-5 March 2020; Publisher: IEEE*Xplore*, **2020**, https://doi.org/10.1109/mwent47943.2020.9067394.

29. Emelyanov, V.M.; Dobrovolskaya, T.A.; Emelyanov, V.V. Three-dimensional Differential XYZ-Y Model for Processing Peasurements of Raman Spectra in the Identification of Gold Nanoparticles on Dielectrics, 2020 Moscow Workshop on Electronic and Networking Technologies (MWENT), Moscow, Russia, 1-5 March 2020; Publisher: IEEE *Xplore*, **2020**, https://doi.org/10.1109/MWENT47943.2020.9067452.
30. Emelyanov, V.M.; Dobrovolskaya, T.A.; Emelyanov, V.V. Solution of multi-dimensional system with XY differentiation of probability density equations for identification of silver nanoparticles on fibers. *IOP Conf. Series: Materials Science and Engineering* **2020**, *905*, https://doi.org/10.1088/1757-899X/905/1/012014.
31. Emelyanov, V.M.; Dobrovolskaya, T.A.; Emelyanov V.V. Identification of silver and gold nanoparticles on the surface of fibers. Multi-dimensional vector-matrix modeling of Raman spectra of textile materials, LAP LAMBERT Academic Publishing, **2017**.